Annals of Biomedical Engineering, Vol. 31, pp. 318–326, 2003
Printed in the USA. All rights reserved.

0090-6964/2003/31(3)/318/9/$20.00

Nonlinear and Frequency-Dependent Mechanical Behavior of the Mouse Respiratory System

HENRIQUE T. MORIYA,[1,2] JOSÉ CARLOS T. B. MORAES,[2] and JASON H. T. BATES[1]

[1]Vermont Lung Center, Department of Medicine and Molecular Physiology and Biophysics, University of Vermont, Burlington, VT and [2]Biomedical Engineering Laboratory, University of São Paulo, São Paulo, Brazil

(Received 12 February 2002; accepted 10 December 2002)

Abstract—The assessment of the mechanical properties of the respiratory system is typically done by oscillating flow into the lungs via the trachea, measuring the resulting pressure generated at the trachea, and relating the two signals to each other in terms of some suitable mathematical model. If the perturbing flow signal is broadband and not too large in amplitude, linear behavior is usually assumed and the input impedance calculated. Alternatively, some researchers have used flow signals that are narrow band but large in amplitude, and invoked nonlinear lumped-parameter models to account for the relationship between flow and pressure. There has been little attempt, however, to deal with respiratory data that are both broadband and reflective of system nonlinearities. In the present study, we collected such data from mice. To interpret these data, we first developed a time-domain approximation to a widely used model of respiratory input impedance. We then extended this model to include nonlinear resistive and elastic terms. We found that the nonlinear elastic term fit the data better than the linear model or the nonlinear resistance model when amplitudes were large. This model may be useful for detecting overinflation of the lung during mechanical ventilation. © *2003 Biomedical Engineering Society.* [DOI: 10.1114/1.1553453]

Keywords—Input impedance, Resistance, Elastance, Frequency domain, Time domain.

INTRODUCTION

The assessment of the mechanical properties of the respiratory system is typically done by oscillating flow into the lungs via the trachea, measuring the resulting pressure generated at the trachea, and relating the two signals to each other in terms of respiratory resistance and elastance.[1,4,5,9,21,22,29,31] Both resistance and elastance depend markedly on the oscillation frequency, and this dependence is most pronounced over the breathing frequency range.[11,23] Consequently, multifrequency analyses of respiratory mechanics are usually performed in the frequency domain through the evaluation of the mechanical input impedance (Z_{in}) of the respiratory system. Z_{in} is most often determined by the forced oscillation technique in which the lungs are perturbed with a broadband flow.[6,7,10–12,23,24,31] The determination of Z_{in} is predicated on the assumption that the respiratory system is linear,[20,23] a requirement which is usually achieved by using small flow amplitudes.

Lutchen and co-workers[14,18] have developed and applied a specially designed broadband flow wave form that serves the dual purpose of ventilating the lungs in a manner sufficient for maintaining gas exchange, while at the same time allowing Z_{in} to be determined up to about 8 Hz. To achieve the first purpose, the peak-to-peak amplitude of this optimal ventilator wave form (OVW) cannot be too small. However, this works against the linearity requirement for the calculation of Z_{in}. Fortunately, the harmonic distortion that arises when a nonlinear system is excited by a broadband input can be minimized by having the frequencies present in the perturbing flow wave form satisfy the no-sum–no-difference (NSND) criterion of Suki and Lutchen.[27] However, this means that all the non-NSND frequencies in pressure arising from the perturbing flow signal are discarded in the determination of Z_{in}. These harmonics could potentially amount to a significant fraction of the total power in pressure, if the system is highly nonlinear.

Our goal was to develop a means of taking nonlinearities into account when the rather large amplitudes of the OVW are applied to the respiratory system. Although, in principle, such an analysis could be performed in the frequency domain, this would involve a complicated series of integrals such as the Volterra series.[16,26,33] We, therefore, undertook our analysis in the time domain because this allowed us to use anatomically based lumped-parameter models that can account for both the nonlinear and multicompartmental behavior of the respiratory system.

METHODS

Experimental Procedures

We studied four normal Balb/c mice weighing 22.4 $\pm$ 0.5 g (mean $\pm$ SD). Each mouse was anesthetized

Address correspondence to Dr. Jason H. T. Bates, University of Vermont, 149 Beaumont Avenue, Burlington, VT 05405-0075. Electronic mail: jhtbates@zoo.uvm.edu

(pentobarbital sodium, 90 mg/kg ip), paralyzed (pancuronium bromide, 1 mg/kg ip), tracheostomized (18 gauge metal cannula), and mechanically ventilated with a tidal volume of 0.25 mL and a breathing frequency of 200 breaths/min using a small animal ventilator (flexiVent, SCIREQ, Montreal, Canada). The flexiVent is a computer-controlled piston pump that can function both as a conventional mechanical ventilator and as a system identification device when its piston is made to follow an appropriate volume displacement wave form.[3,10,25] Positive end-expiratory pressure (PEEP) was set by connecting the expiratory line of the ventilator to a water column.

The animals were ventilated for 6 min periods against three different levels of PEEP (0, 3, and 6 cm H_2O) in random order. At each level of PEEP, the lungs were first inflated twice to a pressure of 25 cm H_2O in order to standardize lung volume history. After an additional minute of regular ventilation, four different amplitudes (0.1, 0.2, 0.3, and 0.4 mL) of the same 8 s broadband volume perturbation were applied sequentially. The different amplitudes were applied in random order with 1.5 min of regular ventilation between each perturbation. After the three PEEP trials were complete, the procedure was repeated at a final PEEP level of 9 cm H_2O. We applied the PEEP of 9 cm H_2O only at the end of the experiment to prevent any resulting overinflation damage to the lung from affecting the measurements at the lower PEEP levels.

Each volume perturbation was applied by interrupting mechanical ventilation, allowing the animal to expire for 1 s against the applied PEEP, and then oscillating the ventilator piston according to the volume perturbation signal. During this procedure, the piston volume displacement (V_{cyl}) and the pressure inside the cylinder (P_{cyl}) were filtered at 300 Hz (six-pole Bessel) and sampled at 1024 Hz. The data were then digitally low-pass filtered (six-pole Bessel) at 30 Hz and decimated to a sampling rate of 128 Hz prior to subsequent analysis.

Volume Perturbation

An OVW-type volume perturbation was generated along the lines originally developed by Lutchen *et al.*[18] First, a set of 50,000 8 s signals was generated. Each signal had the same spectral content; the frequencies of the sinusoidal components spanned the range of 0.5–10.25 Hz and were mutually prime,[7] while the amplitudes decreased hyperbolically with frequency. The phases of each component were chosen randomly. From this initial set of perturbations we selected only those that crossed the mean value four times, corresponding to two breathing cycles. From this subset of signals, we chose the smoothest as the perturbation signal to be used in the present study. Smoothness was measured as the integral of the absolute value of the second derivative of the signal. Finally, the points in the perturbation signal were cyclically permuted so that it began with its minimum value. This ensured that when the signal was applied to an animal's lungs, the resulting changes in lung volume would occur above the lung volume defined by the level of PEEP. This volume perturbation signal was scaled to have peak-to-peak excursions of 0.1, 0.2, 0.3, and 0.4 mL.

TABLE 1. List of symbols and abbreviations.

t	time
V_{cyl}	change of gas volume in flexiVent cylinder
P_{cyl}	pressure in flexiVent cylinder
V	volume change at tracheal opening
$\dot{V}$	flow at tracheal opening
P_{ao}	pressure at tracheal opening
Z_{in}	respiratory input impedance
Z_{ti}	input impedance of respiratory tissues
P_{ti}	pressure across respiratory tissues
f	frequency
R	resistance
G	tissue viscous parameter
H	tissue elastic parameter
I	inertance
α	parameter relating G and H
S	Heaviside step function
Γ	gamma function
R_1	linear resistive constant in nonlinear model
R_2	nonlinear resistive constant in nonlinear model
E	nonlinear elastic parameter
PEEP	positive end-expiratory pressure
i	positive square root of -1
ENV	estimated noise variance
ΔENV	percent change in estimated noise variance
k_d	index of nonlinearity
P_{NI}	power in output signal at frequencies not present in the input signal
P_{TOT}	total power in output signal

Data Analysis

Table 1 lists the symbols and abbreviations used in the following mathematical development. The measured V_{cyl} and P_{cyl} were corrected for gas compressibility within the flexiVent cylinder and for resistive and accelerative losses in the connecting tubing and endotracheal tube as described previously.[3] This yielded the volume (V) and the pressure (P_{ao}) applied directly at the airway opening of the animal. V was differentiated numerically to yield flow ($\dot{V}$) by fitting line segments to each three consecutive points in the signal and taking the slope of the segment as the derivative of the signal at the central point. These data were fit to four models, as follows: (i) the constant-phase model of the lung in the frequency domain, (ii) a time-domain approximation to the constant-phase model, (iii) a time-domain nonlinear extension of the constant-phase model containing a flow-

dependent resistance, and (iv) a time-domain nonlinear extension of the constant-phase model containing a volume-dependent elastance.

We also estimated the degree of nonlinearity in the data in terms of the nonlinear index k_d used by Zhang *et al.*,[32] thus

$$k_d = \sqrt{\frac{P_{\mathrm{NI}}}{P_{\mathrm{TOT}}}}, \tag{1}$$

where P_{TOT} is the total power in the P_{ao} and P_{NI} is the power in P_{ao} at those frequencies not present in the input $\dot{V}$ signal.

Constant-Phase Model

The constant-phase model[12] is described by

$$Z_{\mathrm{in}}(f) = R + i2\pi f I + \frac{G - iH}{(2\pi f)^{\alpha}}, \tag{2}$$

where R is a Newtonian resistance, I is an inertance, G characterizes viscous dissipation of energy in the lung tissues, H characterizes energy storage in the lung tissues, i is the imaginary unit, f is frequency, and

$$\alpha = \frac{2}{\pi}\arctan\left(\frac{H}{G}\right). \tag{3}$$

R has been taken previously to be a useful estimate of overall airway tree resistance,[10] although it may contain a contribution from the chest wall. I reflects mainly the mass of the gas in the central airways.[23] We have shown previously[10] that I is not discernible in data collected from mice below 10 Hz, so henceforth we will neglect the second term in Eq. (2). Although this model was originally proposed specifically to describe the lung,[12] we have also shown that it provides a good description of the entire respiratory system, including the chest wall.[10]

Z_{in} was calculated as described previously.[10,25] The 8 s data records were divided into three 4 s blocks that overlapped by 50%. The first block in each record was discarded and the auto- and cross-power spectra of the remaining two blocks were averaged. The cross-power spectra were then divided by the autopower spectra to yield a transfer function. This transfer function was corrected for the effects of gas compressibility in the ventilator cylinder and the impedance of the channel leading to the animal as described previously.[25] This correction was achieved using dynamic calibration signals of P_{cyl} and V_{cyl} obtained from the flexiVent prior to connecting the animal by applying the volume perturbation through the tracheal cannula first when it was completely closed and then again when it was open to the atmosphere. Finally, the corrected transfer function was divided by $i2\pi f$ to yield Z_{in}.

The constant-phase model [Eq. (2)] was fit to Z_{in} using the following iterative scheme. First, parameter α was set equal to 1.0, and the remaining parameters (R, I, G, and H) were estimated by multiple linear regression. The values of G and H were then used in Eq. (3) to obtain a new value for α. Using this new value for α, the parameters R, I, G, and H were then reestimated by multiple linear regression, allowing a second reestimation of α, and so on. This procedure was repeated ten times (we found that the parameter values typically converged to about four significant figures within five iterations).

Time-Domain Approximation to the Constant-Phase Model

The component of Eq. (2) accounting for the mechanical impedance of the tissues is

$$Z_{\mathrm{ti}}(f) = \frac{G - iH}{(2\pi f)^{\alpha}}. \tag{4}$$

In the time domain this corresponds to an impulse-response function[12,13]

$$z_{\mathrm{ti}}(t) = At^{-k}S(t), \tag{5}$$

where $S(t)$ is the Heaviside step function defined as

$$\begin{aligned} S(t) &= 1, \quad t \geqslant 0, \\ S(t) &= 0, \quad t < 0. \end{aligned} \tag{6}$$

A and k are constants and t is time. G and H are related to A and k as follows:

$$G = A\Gamma(\alpha)\cos\left(\frac{\alpha\pi}{2}\right), \tag{7}$$

$$H = A\Gamma(\alpha)\sin\left(\frac{\alpha\pi}{2}\right), \tag{8}$$

$$k = 1 - \alpha, \tag{9}$$

where $\Gamma(\alpha)$ is the gamma function of α defined as $\int_0^{\infty} t^{\alpha-1}e^{-t}dt$.

$z_{\mathrm{ti}}(t)$ can be rewritten[2]

$$z_{ti}(t)=Ae^{-k\ln(t)}S(t),$$

$$z_{ti}(t)=A\left\{1+[-k\ln(t)]+\frac{[-k\ln(t)]^2}{2!}+\cdots+\frac{[-k\ln(t)]^n}{n!}+\cdots\right\}S(t), \quad (10)$$

$$z_{ti}(t)\approx\{A[1-k\ln(t)]\}S(t),$$

provided the absolute value of $k\ln(t)$ is small compared to unity, where $\ln(t)$ is the natural logarithm of t.

In the frequency domain, the pressure across the tissues due to the applied flow is

$$P_{ti}(f)=\dot{V}(f)Z_{ti}(f), \quad (11)$$

so in the time domain

$$P_{ti}(t)=\dot{V}(t)\otimes z_{ti}(t), \quad (12)$$

where $\otimes$ denotes the operation of convolution. Substituting Eq. (10) into Eq. (12) gives

$$P_{ti}(t)=\dot{V}(t)\otimes\{A[1-k\ln(t)]S(t)\}. \quad (13)$$

But

$$\dot{V}(t)\otimes[AS(t)]=AV(t), \quad (14)$$

and

$$\dot{V}(t)\otimes[Ak\ln(t)S(t)]=Ak\{\dot{V}(t)\otimes[\ln(t)S(t)]\}. \quad (15)$$

Therefore,

$$P_{ti}(t)=AV(t)-Ak\{\dot{V}(t)\otimes[\ln(t)S(t)]\}. \quad (16)$$

By adding a term in R to Eq. (16) we obtain a time-domain approximation to the constant-phase model, thus:

$$P_{ao}(t)=R\dot{V}(t)+AV(t)-Ak\{\dot{V}(t)\otimes[\ln(t)S(t)]\}. \quad (17)$$

In order to use Eq. (17), the signals cannot begin at $t=0$ because $\ln(0)\rightarrow-\infty$. To avoid this situation, we defined all signals as starting at $t=0.01$ s.

A further consideration regarding the use of Eq. (17) is that it is only valid when the magnitude of $k\ln(t)$ is small compared to unity, because only then is the approximation made in the last line of Eq. (10) valid. This obviously is not true in general because $k\ln(t)$ tends to infinity as t tends to infinity and to minus infinity as t tends to zero. Our requirement here is that Eq. (10) holds over the length of our signals, i.e., from $t=0.01-8.01$ s. We tested this by computing $z_{ti}(t)$ in Eq. (10) over this time scale using both the exact expression [first line of Eq. (10)] and its first-order series approximation [last line of Eq. (10)], with a representative value for k of 0.1. We found the two estimates agreed over the 8 s period to within an average of 1.2%, with a standard deviation of 0.9%. Thus, we conclude that the truncated series approximation for $z_{ti}(t)$ is sufficiently accurate for our purposes.

Time-Domain Nonlinear Extensions of the Constant-Phase Model

We extended Eq. (17) in two ways by the addition of *ad hoc* nonlinear terms. The first extension was to add a flow-dependent resistance, thus

$$P_{ao}(t)=R_1\dot{V}(t)+R_2\dot{V}|\dot{V}|+AV(t)-Ak\{\dot{V}(t)\otimes[\ln(t)S(t)]\}, \quad (18)$$

where $|\dot{V}|$ denotes the absolute value of $\dot{V}$ and is required in the above equation because the resistive pressure drop in the lungs reverses sign with a reversal of the direction of $\dot{V}$.

The second extension of the model was to add a volume-dependent elastance term as follows:

$$P_{ao}(t)=R\dot{V}(t)+EV^2(t)+AV(t)-Ak\{\dot{V}(t)\otimes[\ln(t)S(t)]\}. \quad (19)$$

Both nonlinear models [Eqs. (18) and (19)] were fit to the data using multiple linear regression. The convolution in the final term of each equation was calculated using the Euler integration.

Model Comparison

We compared the performances of the time-domain approximation of the constant-phase model [Eq. (17)] and the original frequency-domain formulation [Eq. (2)] in terms of the percentage differences between the parameters R, G, and H estimated by the two models.

The estimated noise variance (ENV) was used as an index of the goodness of fit of the model, where

$$\mathrm{ENV}=\frac{1}{n-m}\sum_{i=1}^{n}(P_i-\hat{P}_i)^2, \quad (20)$$

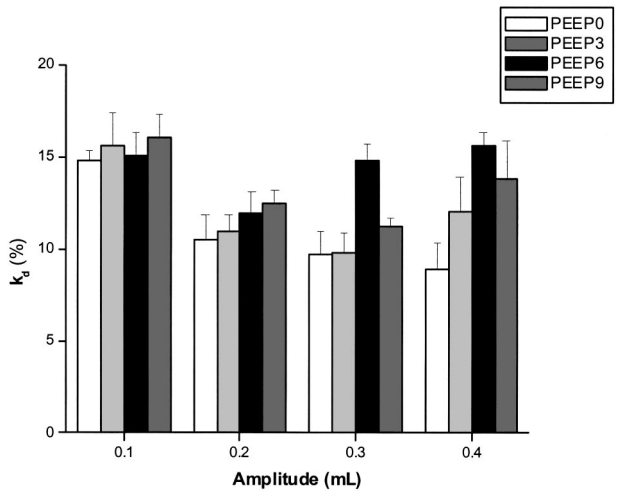

FIGURE 1. Nonlinear index k_d [Eq. (1)].

where P_i is the measured pressure, $\hat{P}_i$ is the pressure predicted by the model, n is the sample size, and m is the number of free model parameters. The lower the value of ENV, the better the model fits the data. When two different models are fit to the same set of data, the model of higher order invariably produces a lower value of ENV. In order to decide if the reduction in ENV is statistically significant, we calculated the percent improvement in ENV, thus

$$\Delta\text{ENV} = 100\left[\frac{\text{ENV}_1 - \text{ENV}_2}{\text{ENV}_1}\right], \qquad (21)$$

where ENV_1 is the larger of the two values of ENV. Provided the noise in the data is normally distributed, the ratio of ENV_1 to ENV_2 follows an F distribution whose number of degrees of freedom is determined by n and the number of parameters in the two models. Using the appropriate F distribution, we determined that if ΔENV is greater than about 30%, then it is less than 5% likely that ENV_1 and ENV_2 are estimates of the same population variance. Thus, when $\Delta\text{ENV} > 30\%$ we concluded that model 2 gave a significantly better fit to the data than did model 1. Otherwise, model 2 was taken as no better than model 1. We must note, however, that the above reasoning is only valid if the residuals between data and model fit are normally distributed. In our case they clearly were not, so we must take the 30% level quoted above as a nominal discriminatory level. From a practical point of view, then, we are interested in values of ΔENV that are either considerably greater than or less than 30%.

RESULTS

Figure 1 shows the nonlinear index k_d [Eq. (1)] for all the tidal volumes and PEEP levels studied. k_d does not depend in any significant way (ANOVA, Tukey post*hoc* comparison) on tidal volume or PEEP.

Table 2 gives the parameter values of the constant-phase model [Eq. (2)] obtained by fitting the model to $Z_{\text{in}}(f)$ in the frequency domain. The percentage differences between the parameters R, G, and H estimated by the constant-phase model [Eq. (2)] and the time-domain approximation of this model [Eq. (17)] were calculated for every combination of tidal volume and PEEP level.

TABLE 2. Values of R, G, and H (mean±standard deviation) for the constant-phase model [Eq. (2)].

Tidal volume	PEEP 0	PEEP 3	PEEP 6	PEEP 9
		R ($\text{cm H}_2\text{O s mL}^{-1}$)		
0.1 mL	0.296±0.116	0.388±0.066	0.349±0.053	0.464±0.038
0.2 mL	0.383±0.113	0.377±0.132	0.429±0.098	0.606±0.052
0.3 mL	0.498±0.248	0.415±0.128	0.509±0.144	0.676±0.080
0.4 mL	0.535±0.250	0.499±0.181	0.705±0.135	0.603±0.119
		G ($\text{cm H}_2\text{O s mL}^{-(1+\alpha)}$)		
0.1 mL	5.174±1.211	3.711±0.678	3.326±0.199	4.807±0.111
0.2 mL	4.331±0.878	3.030±0.678	2.731±0.370	4.324±0.361
0.3 mL	3.630±0.632	2.689±0.669	2.022±0.489	3.883±0.228
0.4 mL	3.433±0.844	2.391±0.601	1.019±0.590	6.027±0.959
		H ($\text{cm H}_2\text{O s mL}^{-(1+\alpha)}$)		
0.1 mL	32.136±9.088	22.678±6.882	20.293±2.406	45.737±4.858
0.2 mL	26.043±4.947	21.735±6.312	23.208±1.979	64.085±7.783
0.3 mL	24.673±3.999	21.548±6.419	31.956±6.787	77.762±9.179
0.4 mL	25.012±8.181	25.144±9.541	47.461±7.825	78.864±7.107

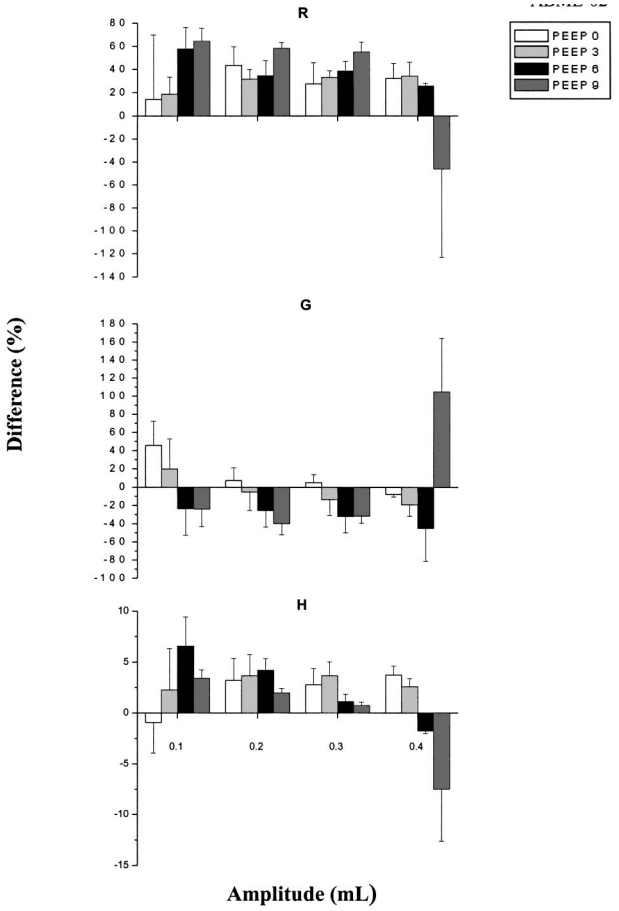

FIGURE 2. Percentage difference between the parameters estimated by the constant-phase model in the frequency domain and the approximation of the constant-phase model in the time domain.

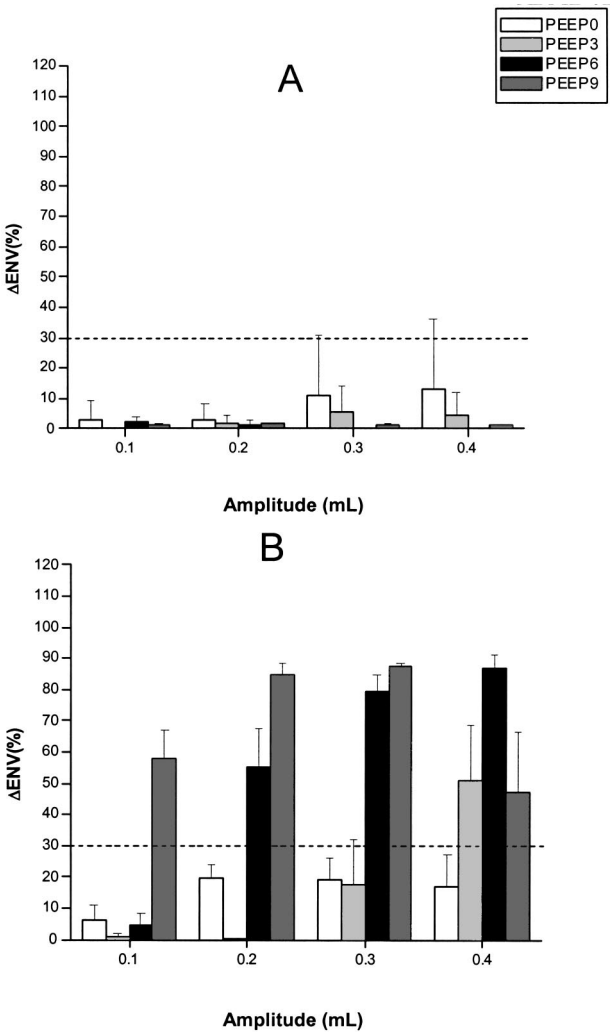

FIGURE 3. Improvement in fit (ΔENV) with the addition of a nonlinear elastance term to the time-domain approximation of the constant-phase model. The horizontal dashed line shows the nominal level above which a value of ΔENV indicates that the nonlinear term produced a significant improvement in the goodness of fit of the model.

The results are shown in Fig. 2. At a tidal volume of 0.4 mL and a PEEP of 9 cm H_2O we suddenly obtained a dramatic change in the differences in the tissue parameters G and H. We suspect this may reflect the onset of overinflation injury, and so we do not consider the data collected under these conditions from now on. For the remainder of the data, the percentage differences in H go from 0.73% at an amplitude of 0.3 mL and PEEP of 9 cm H_2O, to 6.56% at 0.1 mL and 6 cm H_2O. The percentage differences in G go from 5.13% at 0.2 mL and 3 cm H_2O, to 45.81% at 0.1 mL and PEEP of 0 cm H_2O. The lowest percentage difference at R is 14.25% at 0 cm H_2O and 0.1 mL, while the highest percentage difference is 64.43% at 9 cm H_2O and 0.1 mL.

Figure 3 shows how the addition of a nonlinear resistance term [Eq. (18)] and a nonlinear elastance term [Eq. (19)] to the time-domain constant-phase model [Eq. (17)] improves the goodness of fit. ΔENV is shown for each tidal volume and PEEP level investigated. With the nonlinear resistance term [Fig. 3(A)] most cases yielded a value of ΔENV that was far below the nominal 30% significance level. Only the data from the lowest PEEP level at the highest two tidal volumes approached the 30% level. In contrast, the addition of a nonlinear elastance term caused many of the data sets to exceed the 30% ΔENV level substantially [Fig. 3(B)].

DISCUSSION

The use of the constant-phase model to interpret measurements of Z_{in} has gained a wide following recently.[6,10,12,24] However, its use in this regard is predicated on the assumption of linear dynamic behavior from the respiratory system.[20,23] When the imposed oscillations are small, this may be a reasonable assumption. However, nonlinear behavior of respiratory mechanics can become apparent even at normal tidal volumes, es-

pecially when PEEP is elevated.[4,15,21,29,30] Thus, to be comfortable with the assumption of small-amplitude linear behavior, one is compelled to use oscillation amplitudes that are considerably smaller than normal V_T. This constraint cannot, of course, be applied to the OVW, which by definition attempts to deliver a normal V_T. Lutchen *et al.*[18] employ a cunning technique for dealing with nonlinearities when using the OVW by having the OVW contain only components satisfying the no-sum–no-difference criterion[27] and then calculating Z_{in} only at those frequencies present in the input $\dot{V}$ wave form. This means that any harmonics in P_{ao}, produced by passing $\dot{V}$ through a nonlinear system, are discarded. The problem with this approach is that if the nonlinearities are strong, then a significant amount of information about the system is not being used in its assessment.

The parameters of the constant-phase model [Eq. (2)] vary with PEEP and tidal volume (Table 2) in characteristic ways. For example, H is minimal at an intermediate PEEP level (3 cm H_2O at three of the tidal volumes investigated and 6 cm H_2O at the remaining tidal volume). This has been described before[10] and is thought to be due to strain stiffening of the tissues at higher PEEPs and to some degree of airspace closure at PEEP 0. G shows a somewhat similar pattern, no doubt for the same reasons. R shows a more curious pattern of increasing with both PEEP and tidal volume. If R really is a measure of airway resistance, one might expect the opposite to occur as the airways increase in caliber with increasing lung volume. However, it is possible that our R values include some contribution from the chest wall (this might be more apparent in mice than other species, as mice have relatively large airways for their lung size,[10] which could make the effect of their tissues on R relatively more important than in other species).

Our goal was to develop a method for encapsulating the mechanical behavior of the respiratory system in a way that retains at least some of the nonlinear information present in the measured pressure–flow relationships. We could have attempted this in the frequency domain in terms of a Volterra series.[16,26,33] However, this series can rapidly become intractable, and interpreting its various terms physiologically is generally not possible. Suki *et al.*[28] investigated an alternative approach in which they fit block-structured nonlinear models in the time domain to data from dogs. Maksym and Bates[19] applied a similar approach to data from rat lungs. Again, however, it is not obvious how to interpret the elements of these models in physiologic terms. Also, the fitting process is somewhat computationally expensive, requiring iteration between the time and frequency domains. Therefore, we decided to develop nonlinear frequency-dependent lumped-parameter models in the time domain. These models are derived from a linear frequency-domain model whose utility and interpretation are well established.[10,12,24] Also, by expressing the models in terms of a truncated exponential expansion [Eq. (10)], we were able to cast them in a form that can be fit to data using multiple linear regression [Eqs. (17), (18), and (19)]. This poses a relatively low computational burden. Finally, even though the data analyzed in the present study were collected under steady-state conditions, Eqs. (17), (18), and (19) can be fit using recursive least squares.[17] This would allow them to be applied to nonstationary data in order to track changing parameter values.

The first step in this process was recasting the linear constant-phase model in the time domain. This was not straightforward because the constant-phase model has an impulse response that is infinite at $t=0$. Therefore, we resorted to a time-domain approximation to the constant-phase model that employs convolution with the first two terms of the series expansion for a power series, and we started the impulse response at $t=0.01$ s in order to avoid singularities. We then had to address the issue of how equivalent the two model formulations are. The frequency- and time-domain versions of the constant-phase model weight the data differently when estimating the model parameters. That is, minimizing the squared residuals between a predicted and calculated Z_{in} is not equivalent to minimizing the residuals between measured and estimated P_{ao}. Consequently, any errors in either the data or the models would be expected to affect the parameters differently in the two domains. We thus might also expect that differences in the model parameter obtained in the two domains should increase with the degree of nonlinearity in the data. At the very highest level of PEEP and tidal volume the parameter differences are opposite in sign to most of the other cases. We suspect this may have been due to a change in the state of the lung induced by overdistension; it was our impression that the mice did not do well being ventilated under these conditions, which is why we always applied the highest PEEP and tidal volume after the other data had been collected. For the remaining data in Fig. 2, there is a suggestion that the parameter differences increase with PEEP, however, the effect is not marked so we cannot draw any firm conclusions.

The parameter H, which characterizes energy storage in the tissues, had the lowest percentage differences between the frequency- and time-domain models (Fig. 2). This can be explained by the fact that most of the P signal produced by the perturbations reflected stored elastic energy, because most of the power in V was at low frequencies. Consequently, H is most strongly determined by the data and so has the greatest signal-to-noise ratio. In contrast, the highest percentage differences occurred in R, which is the asymptotic value of the real part of the impedance as frequency goes to infinity. R is

thus the parameter least strongly determined by the data, and so it tends to have the lowest signal-to-noise ratio. Nevertheless, the two models produce parameter values that are at least comparable over the range of conditions we investigated.

The second step in our model development was to add the capacity for the time-domain constant-phase model to account for nonlinearities. Previous studies[4,15,21,30] have shown that the most important nonlinearity to appear during mechanical ventilation is invariably a volume-dependent elastance. Therefore, we added an *ad hoc* term in V^2 to our model [Eq. (19)]. We then assessed the necessity for this extra term, in any particular case, by examining how much it improved the fit to the data. We found that the fit was improved significantly as both V_T and PEEP increased [Fig. 3(B)]. This is explicable on the basis that the respiratory tissues assume progressively stiffening behavior as lung volume is increased, causing their pressure–volume properties to become increasingly nonlinear.[4,8,15,21,30] We also examined the effect of adding a flow-dependent resistance term to the time-domain model [Eq. (18)]. In most cases, this had a minimal effect on ΔENV [Fig. 3(A)]. Interestingly, ΔENV obtained with the flow-dependent resistance was largest at the two highest tidal volumes and lowest PEEP level [Fig. 3(A)]. This is consistent with the notion that turbulent flow in the airways would most likely occur when the highest gas flows (produced by the high tidal volumes) pass through narrowed airways (i.e., at the lowest lung volume).

In conclusion, our study has shown that in normal mice, ventilation with the OVW produces mechanical behavior that becomes significantly nonlinear as PEEP and V_T are increased. Although these nonlinearities can be neglected using a perturbation wave form designed to avoid harmonic distortion, doing so may discard a significant and interesting portion of the data. In particular, by keeping track of the appearance of a volume-dependent nonlinearity, one may be able to detect overinflation of the lung, or the onset of pathologies that cause the lung tissues to acquire nonlinear elastic behavior at lower than normal volumes.

ACKNOWLEDGMENTS

This work was supported by NIH Grant Nos. R01HL62746, R01HL67273, and NCRR COBRE P20RR15557, and a grant from Conselho Nacional de Desenvolvimento Cientifico e Tecnológico (CNPq), Brazil.

REFERENCES

[1] Antonaglia, V., A. Peratoner, L. Simoni, A. Gullo, J. Milic-Emili, and W. A. Zin. Bedside assessment of respiratory viscoelastic properties in ventilated patients. *Eur. Respir. J.* 16:302–308, 2000.

[2] Bates, J. H. T., G. N. Maksym, D. Navajas, and B. Suki. Lung tissue rheology and 1/f noise. *Ann. Biomed. Eng.* 22:674–681, 1994.

[3] Bates, J. H. T., T. F. Schuessler, C. Dolman, and D. H. Eidelman. Temporal dynamics of acute isovolume bronchoconstriction in the rat. *J. Appl. Physiol.* 82:55–62, 1997.

[4] Bersten, A. D. Measurement of overinflation by multiple linear regression analysis in patients with acute lung injury. *Eur. Respir. J.* 12:526–532, 1998.

[5] Bijaoui, E., S. A. Tuck, J. E. Remmers, and J. H. T. Bates. Estimating respiratory mechanics in the presence of flow limitation. *J. Appl. Physiol.* 86:418–426, 1999.

[6] Bijaoui, E., P. F. Baconnier, and J. H. T. Bates. Mechanical output impedance of the lung determined from cardiogenic oscillations. *J. Appl. Physiol.* 91:859–865, 2001.

[7] Daróczy, B., and Z. Hantos. Generation of optimum pseudorandom signals for respiratory impedance measurements. *Int. J. Bio-Med. Comput.* 25:21–31, 1990.

[8] Dechman, G., A.-M. Lauzon, and J. H. T. Bates. Mechanical behavior of the canine respiratory system at very low lung volumes. *Respir. Physiol.* 95:119–129, 1994.

[9] Farré, R., M. Mancini, M. Rotger, M. Ferrer, J. Roca, and D. Navajas. Oscillatory resistance measured during noninvasive proportional assist ventilation. *Am. J. Respir. Crit. Care Med.* 164:790–794, 2001.

[10] Gomes, R. F. M., X. Shen, R. Ramchandani, R. S. Tepper, and J. H. T. Bates. Comparative respiratory system mechanics in rodents. *J. Appl. Physiol.* 89:908–916, 2000.

[11] Hantos, Z., B. Daróczy, B. Suki, G. Galgóczy, and T. Csendes. Forced oscillatory impedance of the respiratory system at low frequencies. *J. Appl. Physiol.* 60:123–132, 1986.

[12] Hantos, Z., B. Daróczy, B. Suki, S. Nagy, and J. J. Fredberg. Input impedance and peripheral inhomogeneity of dog lungs. *J. Appl. Physiol.* 72:168–178, 1992.

[13] Hildebrandt, J. Comparison of mathematical models for cat lung and viscoelastic balloon derived by Laplace transform methods from pressure–volume data. *Bull. Math. Biophys.* 31:651–667, 1969.

[14] Kaczka, D. W., E. P. Ingenito, B. Suki, and K. R. Lutchen. Partitioning airway and lung tissue resistances in humans: Effects of bronchoconstriction. *J. Appl. Physiol.* 82:1531–1541, 1997.

[15] Kano, S., C. J. Lanteri, A. W. Duncan, and P. D. Sly. Influence of nonlinearities on estimates of respiratory mechanics using multilinear regression analysis. *J. Appl. Physiol.* 77:1185–1197, 1994.

[16] Korenberg, M. J., and I. W. Hunter. The identification of nonlinear biological systems: Volterra kernel approaches. *Ann. Biomed. Eng.* 24:250–268, 1996.

[17] Lauzon, A.-M., and J. H. T. Bates. Estimation of time-varying respiratory mechanical parameters by recursive least squares. *J. Appl. Physiol.* 71:1159–1165, 1991.

[18] Lutchen, K. R., K. Yang, D. W. Kaczka, and B. Suki. Optimal ventilation wave forms for estimating low-frequency respiratory impedance. *J. Appl. Physiol.* 75:478–488, 1993.

[19] Maksym, G. N., and J. H. T. Bates. Nonparametric block-structure modeling of rat lung mechanics. *Ann. Biomed. Eng.* 25:1000–1008, 1997.

[20] Michaelson, E. D., E. D. Grassman, and W. R. Peters. Pul-

monary mechanics by spectral analysis of forced random noise. *J. Clin. Invest.* 56:1210–1230, 1975.
[21] Muramatsu, K., K. Yukitake, M. Nakamura, I. Matsumoto, and Y. Motohiro. Monitoring of nonlinear respiratory elastance using a multiple linear regression analysis. *Eur. Respir. J.* 17:1158–1166, 2001.
[22] Pelosi, P., M. Croci, I. Ravagnan, M. Cerisara, P. Vicardi, A. Lissoni, and L. Gattinoni. Respiratory system mechanics in sedated, paralyzed, morbidly obese patients. *J. Appl. Physiol.* 82:811–818, 1997.
[23] Peslin, R., and J. J. Fredberg. Oscillation mechanics of the respiratory system. In: Handbook of Physiology. Mechanics of Breathing, edited by P. T. Macklem and J. Mead. Bethesda, MA: American Physiological Society, 1986, pp. 145–177.
[24] Peták, F., W. Habre, Z. Hantos, P. D. Sly, and D. R. Morel. Effects of pulmonary vascular pressures and flow on airway and parenchymal mechanics in isolated rat lungs. *J. Appl. Physiol.* 92:169–178, 2002.
[25] Schuessler, T. F., and J. H. T. Bates. Computer-controlled research ventilator for small animals: Design and evaluation. *IEEE Trans. Biomed. Eng.* 42:860–866, 1995.
[26] Suki, B., and J. H. T. Bates. A nonlinear viscoelastic model of lung tissue mechanics. *J. Appl. Physiol.* 71:826–833, 1991.
[27] Suki, B., and K. R. Lutchen. Pseudorandom signals to estimate apparent transfer and coherence functions of nonlinear systems: Applications to respiratory mechanics. *IEEE Trans. Biomed. Eng.* 39:1142–1151, 1992.
[28] Suki, B., Q. Zhang, and K. R. Lutchen. Relationship between frequency and amplitude dependence in the lung: A nonlinear block-structured modeling approach. *J. Appl. Physiol.* 79:660–671, 1995.
[29] Vassiliou, M. P., L. Petri, A. Amygdalou, M. Patrani, C. Psarakis, D. Nikolaki, G. Georgiadis, and P. K. Behrakis. Linear and nonlinear analysis of pressure and flow during mechanical ventilation. *Intensive Care Med.* 26:1057–1064, 2000.
[30] Wagers, S., L. Lundblad, H. T. Moriya, J. H. T. Bates, and C. G. Irvin. Nonlinearity of respiratory mechanics during bronchoconstriction in mice with airway inflammation. *J. Appl. Physiol.* 92:1802–1807, 2002.
[31] Zerah, F., A. M. Lorino, H. Lorino, A. Harf, and I. Macquin-Mavier. Forced oscillation technique versus spirometry to assess bronchodilatation in patients with asthma and COPD. *Chest* 108:41–47, 1995.
[32] Zhang, Q., K. R. Lutchen, and B. Suki. Harmonic distortion from nonlinear systems with broadband inputs: Applications to lung mechanics. *Ann. Biomed. Eng.* 23:672–681, 1995.
[33] Zhang, Q., K. R. Lutchen, and B. Suki. A frequency-domain approach to nonlinear and structure identification for long memory systems: Application to lung mechanics. *Ann. Biomed. Eng.* 27:1–13, 1999.